

Improving the efficiency of a portable room-temperature CZT gamma-Ray spectrometer

Yves A Ramirez

Electrical & Computer Engineering, University of Texas at El Paso, El Paso, TX, 79968

1) Abstract. - We have characterized a high-resolution room temperature gamma-ray detector module based on a 4x4 array of Cadmium-Zinc-Telluride (CZT) crystals with improved performance and energy resolution. The detectors can compensate for crystal defects and eliminate the necessity of buying high quality crystals at excessive costs to obtain a higher energy resolution. Lifetime and leakage current measurements were performed on the CZT crystal detectors. To ensure that the crystals used in the arrays were fit for the task, the crystals were tested for carrier lifetime and leakage current, before testing the finished device and comparing its results with those of a High-purity Germanium (HPGe) detector. To measure carrier lifetime, two tests were performed: Time-of-Flight, which measures carrier drift time and amplitude, and spectroscopy to identify peak position and calculate lifetime through Hecht's equation. Leakage current was measured in the bulk and surface of the crystals to analyze losses and noise in the collected data due to defects in the crystals, and they are compared to the leakage current of the whole crystals to see at what part of the crystal does most of the leakage current come from. The module was assembled and tested by identifying the following radioactive sources: ^{137}Cs , ^{241}Am , ^{238}U , and ^{232}Th . The radiation peaks were identified using Cambio software. Test results were plotted in OriginLab analyze the relation between amplitude and drift time on Time of Flight measurements, the relation between applied voltage and peak position in Hecht's equation measurements, and the relation between applied voltage and amplitude of leakage current in leakage current measurements. Interactive Data Language (IDL) was used to calculate the carrier lifetime of the crystals, their resistivity, sensitivity, and to analyze the data given by the detector. A brick of unknown composition was used for shielding, and after realizing that it was radioactive, it was analyzed by the detector and the results were compared with those of a HPGe detector used on the same brick. The brick serves as a proof of the efficiency of the detector and all the potential applications it has.

2) Introduction. -Illicit radioactive sources are a significant risk for national security due to their applications in the fabrication of weapons of mass destruction. The Treaty on the Non-Proliferation of Nuclear Weapons (NPT) was established with the purpose of preventing the spread of nuclear weapons and promote peaceful uses of nuclear technology between countries. We now know that not all countries that signed the treaty are compliant, which makes radiation detection crucial for nonproliferation objectives. Semiconductor-based radiation detectors were developed in the early 1960s and in recent years have come up as a viable alternative to the gas-filled detectors previously used, offering high energy resolution at a more compact size and lower cost. Popular semiconductor materials used for semiconductor radiation detectors are Silicon (Si) and Germanium (Ge). High-Purity Ge detectors are currently the detectors with the highest energy resolution available in the market, however they are expensive and require cryogenic cooling to operate at high efficiency. Cadmium-Zinc-Telluride (CZT) has come up as an excellent alternative for semiconductor radiation detectors due to its ability to perform at room temperature and high-energy resolution achievable at room temperature. However, the crystal growing process for CZT produces a high quantity of defected crystals, making high-purity crystals only available at higher costs. This prototype offers a solution to the excessive cost of CZT detectors by working with 4x4 arrays of mid-quality crystals using a Virtual Frisch-Grid (VFG) technique to improve their electron mobility.

3) Detector Design

CZT Crystals as Semiconductor Radiation Detectors. – Semiconductors offer several advantages for radiation detection; they offer higher energy resolution at a lower cost and compact size when compared to gas-filled detectors. The most popular semiconductor materials for radiation materials are Silicon (Si) and Germanium (Ge), being High-Purity Ge (HPGe) detectors the ones with highest energy resolution. However, HPGe detectors require cryogenic cooling to offer high performance, this increases both the size and cost of the detector. CZT recently came up as a viable replacement to Ge for Gamma-Ray spectroscopy. A viable alternative to HPGe is CZT. The bandgap values for CZT are large enough to allow for room-temperature operation [1]. This eliminates the need for cryogenic cooling, replacing it for modest cooling to reduce leakage current [1]. This advantage reduces detector size and cost greatly.

When a large electric field is applied through the detector and a high-energy particle interacts with the crystal, electron-hole pairs are created and charges drift across the depletion region (in this case the whole crystal). In this case, the electric field is produced by applying a high voltage across the detector (2500-3000 V) and the charges are collected at the anode of the detector. A drawback from all the advantages offered by CZT is that the growth technique for the crystals produces a large number of defected crystals compared to the high-purity crystals produced. This increases the cost of the high-purity crystals, dramatically increasing the cost of the detector.

Detector Module. – This Gamma camera was designed to give use to the mid or low-quality crystals, therefore decreasing the cost of the detector, but having high energy resolution at the same time by creating arrays of the defected crystals. The crystals used for the detectors were $6 \times 6 \times 20 \text{mm}^3$ bars of CZT crystal encapsulated in an ultrathin polyester shell with four charge-sensing pads placed near the anode of the detectors for X-Y coordinate measurements and spring contacts on both the anode and cathode for charge collection (fig. 1).

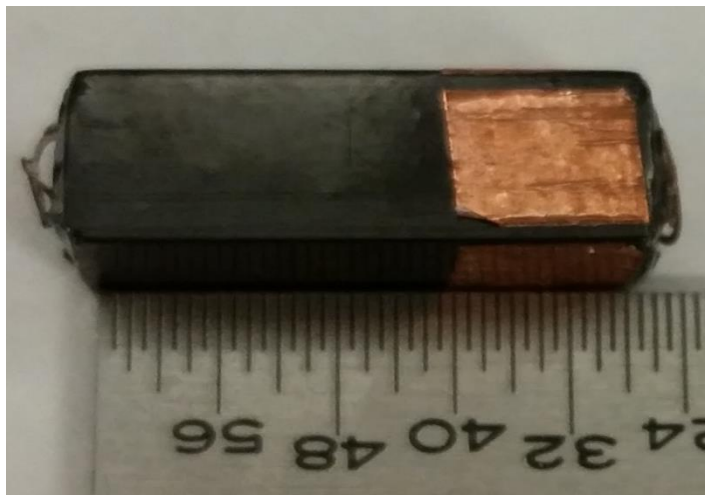


Figure 1. CZT detector

The detectors are placed in 4x4 arrays with interconnected pads that offer higher energy resolution (the resolution is improved as the number of detectors in the array increases)

connected to a high-voltage cable to produce a large electric field across the detectors. The array is connected through a multipin board to an Application Specific Integrated Circuit (ASIC) that consists of a preamplifier since the collected signal is in the μA scale, a shaping amplifier, an analog-to-digital converter (ADC) to convert peak amplitudes in time to digital signals, and low-voltage passive converters for power. The ASIC motherboard is connected to a Field Programmable Gate Array (FPGA) for data analysis and communication with ASIC via USB interface [2] (fig. 2).

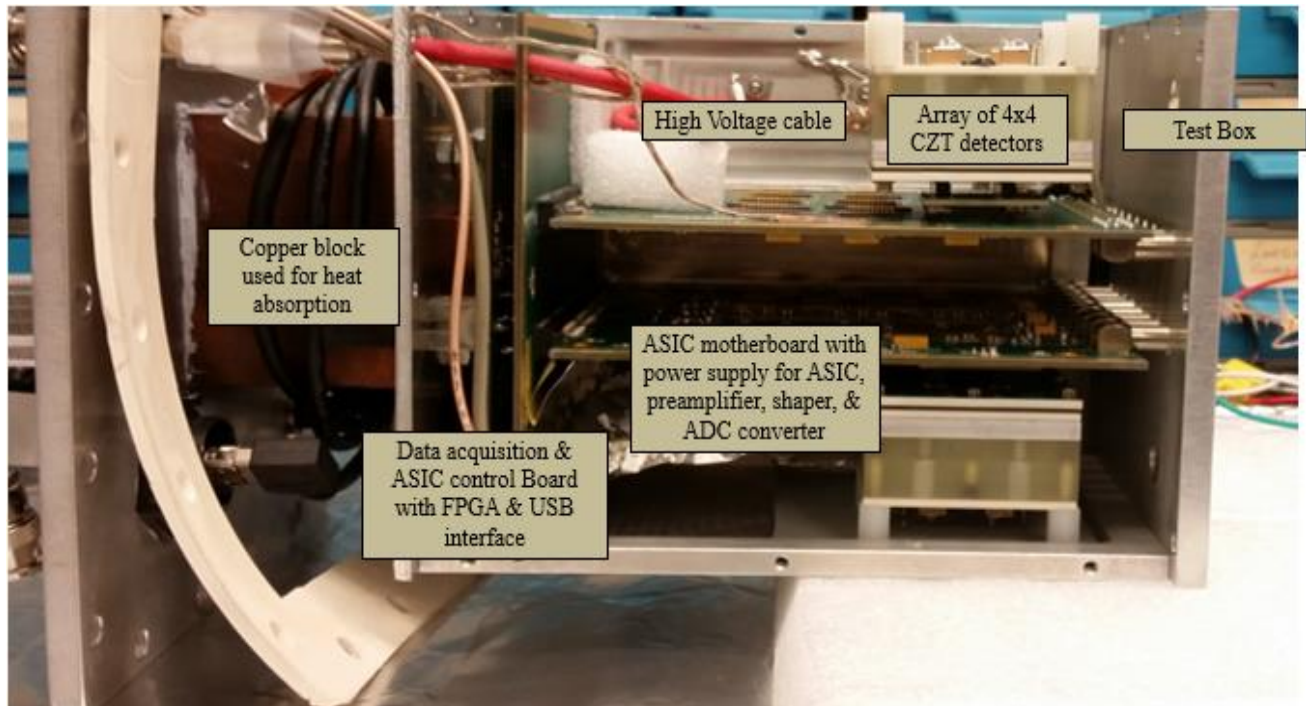


Figure 2. Sideview of the Gamma camera showing inside components.

Moderate cooling is used to reduce leakage current [1]. A copper rod is connected to a test box that houses the system to absorb heat. The outer flange is connected to a Peltier module, a heat sink, and a fan. Temperature is also monitored inside the environmental box and on the ASIC. Special wrapping is used avoid moisture condensation. The entire system is enclosed in a test box that houses the HV cable, the arrays, the ASIC, and the FPGA inside a secondary 3-D printed box used to protect the system from environmental damage and is designed so that tungsten plates can be placed at each side of the system to provide shielding from background noise (fig. 3).



Figure 3. Cooling system attached to detector and outside box.

The system is connected through the FPGA to an external computer where, using custom software, data can be extracted in real time, the readings of all the detectors can be monitored, the ASIC can be controlled, and calibrations can be made. After each test, the acquired data is taken to pass it through 3-D corrections separately using Interactive Data Language (IDL) (fig. 4).



Figure 4. Detector reading display.

4) Tests and Measurements

Lifetime Measurements. – Carrier lifetime is the time it takes for a charge carrier to recombine once it has started drifting. Carrier lifetime varies depending on the conditions of the semiconductor device. It is important to have the highest lifetime possible to collect the most amount of charge possible. It is also important to know the lifetime of the of the crystals that will be used as detectors in the Gamma camera, the highest purity crystals are the ones with the greatest lifetimes, but since the idea is to avoid the need to buy high quality crystals, the crystals with the greatest lifetime within the desired quality range must be selected to be placed in the arrays. To identify the detectors with the greatest lifetimes, they are subject to two different techniques of lifetime measurements: Time-of-Flight, and Hecht's equation.

In Time-of-Flight measures the time it takes for a particle to travel through a medium, in this case, the time it takes for a charge to travel through the entire length of the CZT crystal. The detector is placed in a special container, a guard ring is used to ground the detector from one end, wrapping the detector from the anode until around half of it is covered, and an adjustable probe is in the other end where the voltage will be applied (fig. 5). The container is connected to a

voltage source and an oscilloscope. A voltage is applied to produce an electric field through the detector and a radioactive source is placed on top of the container. In this case, ^{137}Cs . The source produces a signal in the detector which is measured by the oscilloscope with respect to time. Since the measured amplitude is a voltage that flows through the whole detector, the time it takes to reach said amplitude, called “drift time” is the time it takes for the carrier to flow through the detector, and it is inversely proportional to carrier lifetime. For this measurement, different values of voltage were applied to see the response of the detector at different voltages. The amplitude of the signal increases when the applied voltage increases, and as the amplitude increases, the drift time value decreases. Since the relation between drift time and carrier lifetime is inversely proportional, as drift time decreases, the lifetime value increases.

Hecht’s equation measurements consist of using Gamma-Ray spectroscopy to obtain the value of $\mu\tau$ (mobility times lifetime) for carriers in that detector from the plot of the energy peak position at a certain applied voltage. For this measurement, the setup is almost the same that for Time-of-Flight except that ^{137}Cs is replaced by ^{241}Am due to it being the best source for calibration and the reading is displayed as spectroscopy readings showing the position of the main peak of the radiation source at a certain value of counts depending on the applied voltage. Once that raw data is obtained, it is inputted in an IDL program that calculated the $\mu\tau$ product and the individual values of each parameter through Hecht’s equation.

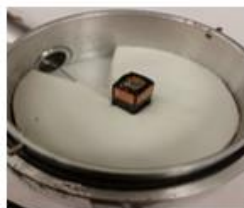


Figure 5. Detector mounted on testing container.

Leakage Current Measurements. – Leakage current measurements are just as important for as lifetime measurements to determine the quality of the detectors. Leakage current represents defects in the crystals of the detectors and the larger it is, the larger is the noise in the collected signals as well as signal loss. The larger voltage applied to the crystals, the larger the leakage current, and since voltages applied to semiconductor detectors to obtain electric field are in the KV scale, leakage current can be quite large. Leakage current for a 1mm thick bulk silicon detector with a 1cm^2 area and an applied bias of 500 V is roughly 0.1A. Considering that current pulses collected from the detectors are in the μA scale, it is important to keep leakage current to a minimum or resistivity as high as possible. Acceptable values for leakage current must be kept at a maximum of a nanoamp, and the ideal value should be in the picoamp scale. To measure leakage current, the detector is placed in a test box where voltage is applied to the cathode of the detector and the anode is grounded (fig. 6). The current is measured by a digital multimeter controlled by a C++ program, where the data is plotted in IDL software to obtain the values for resistivity. The resistivity values should be $>10^{10}\ \Omega\cdot\text{cm}$ for the detector to be fit for an array. Leakage current was measured in the entire crystal bars, as well as the surface, and the bulk of

the crystals separately to determine where in the crystals does most of the leakage current comes from.

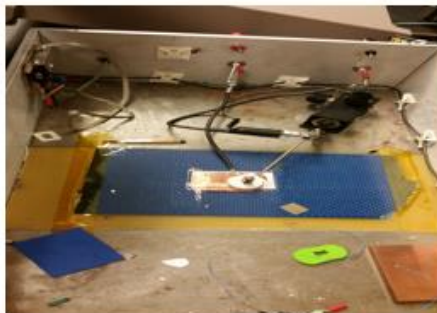


Figure 6. CZT detector mounted on testing box for leakage current measurements.

Detector Testing. – Once the entire system is assembled, it is connected to the control computer and the power supplies. To test the Gamma camera, the detectors are calibrated using a source and then the source is placed at a specific location near the arrays for the camera to identify the peaks of the source (fig. 7). The detector was tested with ^{137}Cs , ^{241}Am , ^{238}U , and ^{232}Th , as well as a U ore, and a regular plate with radioactive paint. The sources were at first placed right above the arrays, then to the sides and beneath the detector. After those tests, the sources were placed at longer distances to test the range of the detector. The maximum distance the source was separated from the detector for testing was of around 1.6 meters, but it is not the range limit of the detector. The sources were also placed at 45° and 60° angles. Tungsten plates were also used in some of the tests for background noise shielding. The results of each test were compared to obtain the sensitivity of the detector which was calculated by obtaining the minimum time for a peak to be detected. When measuring a source, the spectrum measured by each of the 16 detectors in the array is displayed (fig. 12), as well as the spectrum of the entire array (fig. 13), this helps to see if how every detector is performing and to do the appropriate calibrations. The raw data is extracted after each test to go through 3-D corrections. After the corrections, the measured spectrum can be shown with a much higher energy resolution.



Figure 7. Detector tested on a ^{238}U source.

Yoda the Brick. – As a test, we conducted spectroscopic measurements of a special brick used as a shielding element. The brick was turned out to be a slightly radioactive source (fig. 8). The brick went through several tests and its spectrum was analyzed to identify the sources in it. After doing the analysis with the Gamma camera, the same brick was measured by a HPGe detector to compare the results of both measurements. Peak identification was done with the spectra of both detectors to identify the sources present in the brick. The brick was nicknamed “Yoda”



Figure 8. Detector module tested on “Yoda the Brick”.

5) Results. – Time-of-Flight measurements proved to show greater results compared with Hecht for lifetime measurements. Time-of-Flight calculated a maximum carrier lifetime of $228 \mu\text{s}$ (fig. 8), while Hecht’s equation limitations put a limit in lifetime value of $10.1 \mu\text{s}$ (fig. 9). Time-of-Flight measurements results turned out positive as $228 \mu\text{s}$ is a long enough lifetime for electrons to be captured by the detectors.

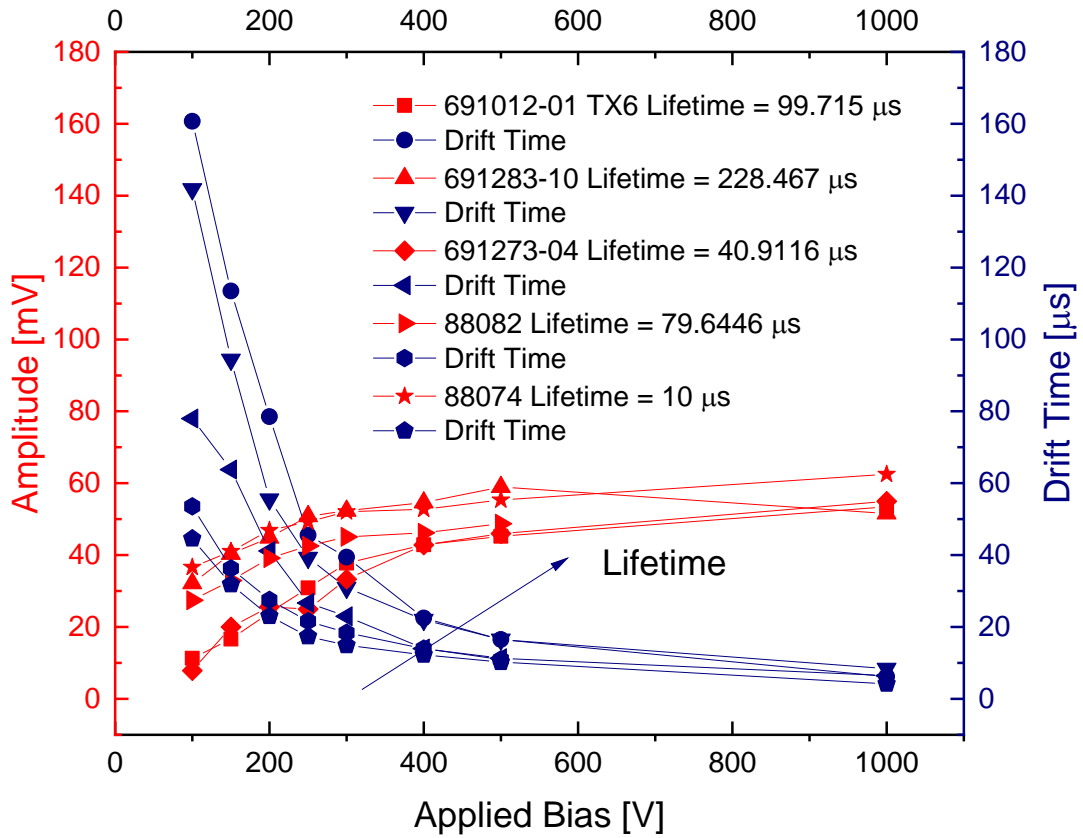


Figure 8. Graph of amplitude of measured signal and drift time with respect to applied voltage on several detectors

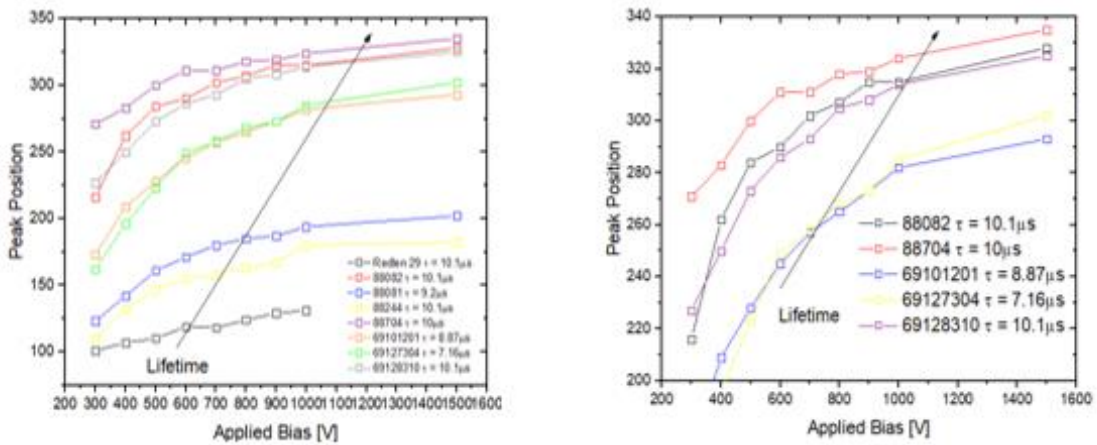


Figure 9. Graphs of Hecht's equation measurements on all detectors (left) and only those with proficient lifetimes (right).

Results for leakage current were diverse. Different detectors showed resistivity in the scale of $10^{11} \Omega \cdot \text{cm}$ which is a desirable value for resistivity and others $10^{10} \Omega \cdot \text{cm}$ which can produce large leakage current (fig.10). Measurements of bulk and surface measurements showed that most of the leakage current in the detectors is generated at the surface, this could be due to defects in the crystals that appear when they are cut into bars, or damage from encapsulation.

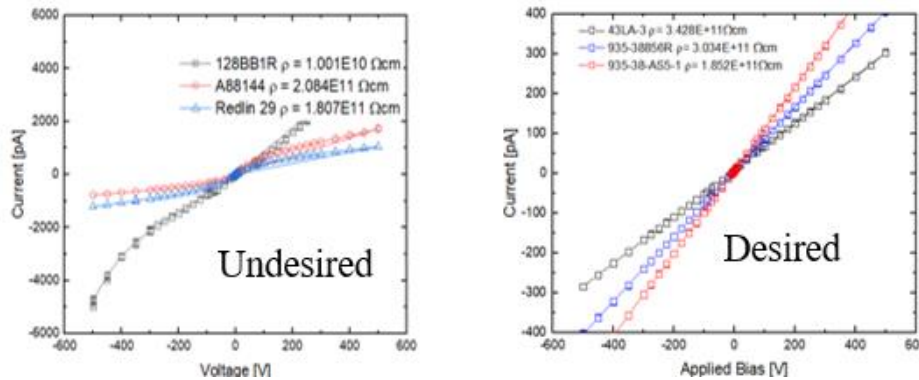


Figure 10. Low resistivity detectors with high leakage current (left). High resistivity detectors with low leakage current (right).

The testing of the entire module showed that the Gamma camera can successfully identify different radioactive sources at different distances and positions operating at room temperature with high energy resolution. Sensitivity measurements show that the minimum time for peak detection is ~ 6 seconds. 3-D corrections can increase energy resolution from a Full Width Half-Max (FWHM) of 2.5% before corrections to up to a FWHM of 0.9% for a 662 KeV peak (^{137}Cs peak) after corrections (fig. 11). This result is very promising considering that the best energy resolutions in radiation detectors is of $\text{FWHM} < 1\%$.

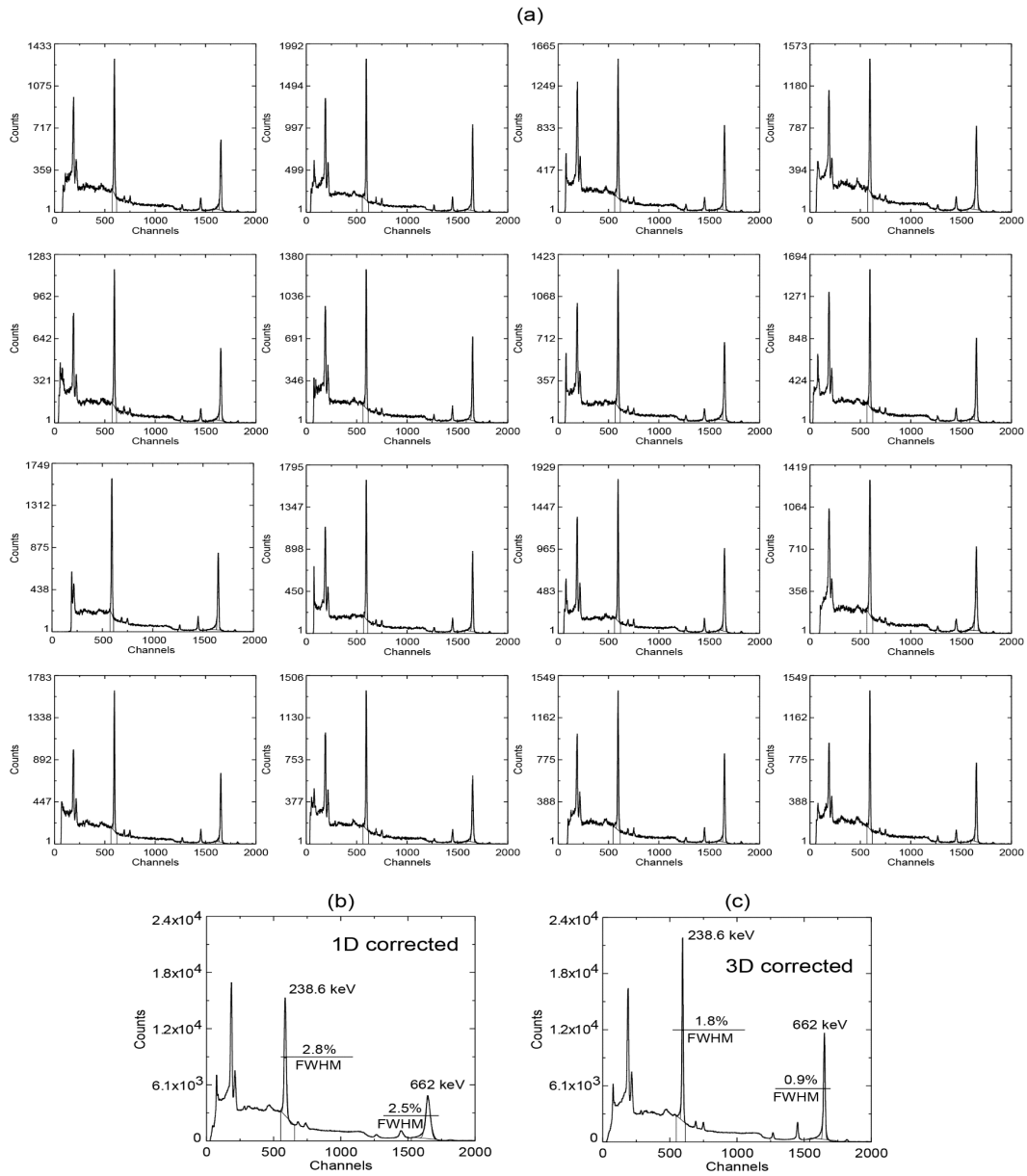


Figure 11. (a) spectra measured from 16-detectors after 3D corrections, (b) the combined spectra after 1D and (c) after 3D corrections.

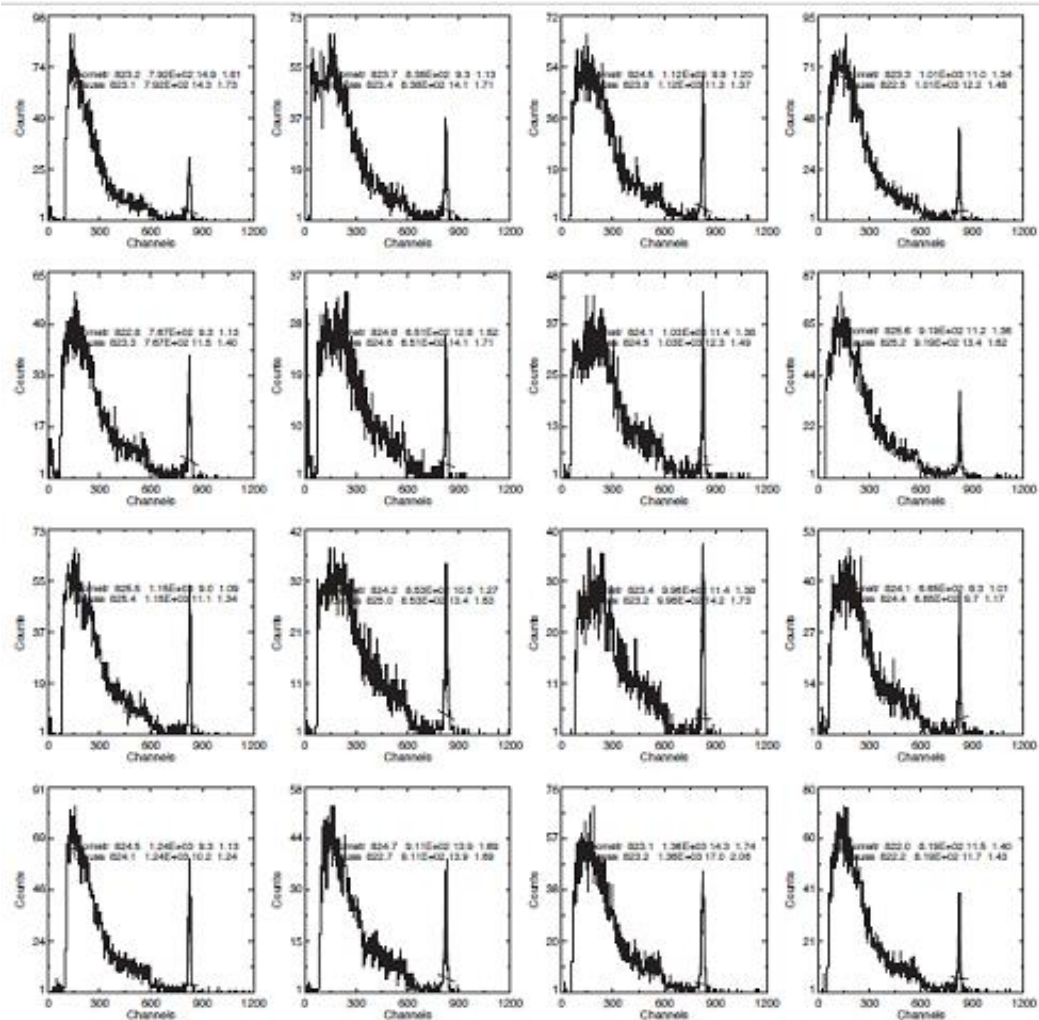


Figure 12. ¹³⁷Cs spectrum at 1m distance measured by all detectors in array

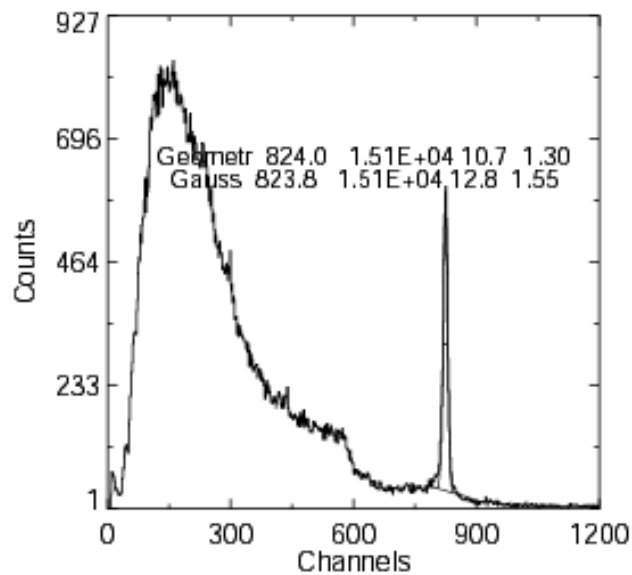


Figure 13. Final spectrum obtained by the array

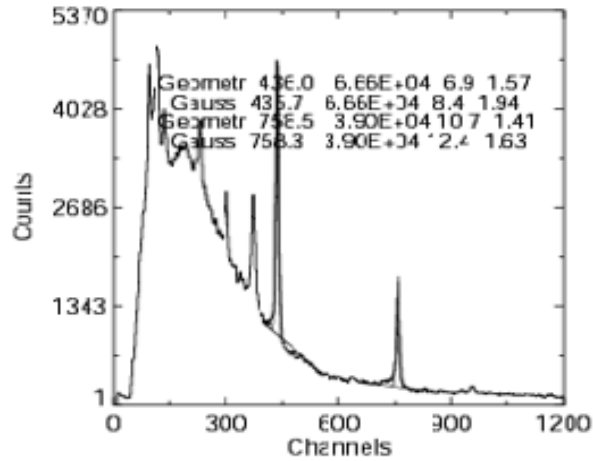


Figure 14. U ore spectrum.

After the 3-D corrections were applied to the spectrum of the brick obtained from the CZT detector and obtaining the spectrum from the HPGc detector, the energy peaks showed that the sources in the brick were ^{232}Th and ^{238}U ore for the most part. This lead to the conclusion that the brick contained ^{238}U at first, and it started to decay into ^{232}Th (fig 15). The comparison with the HPGc detector served to determine the efficiency of the CZT camera, as both detectors were able to identify the sources in the brick.

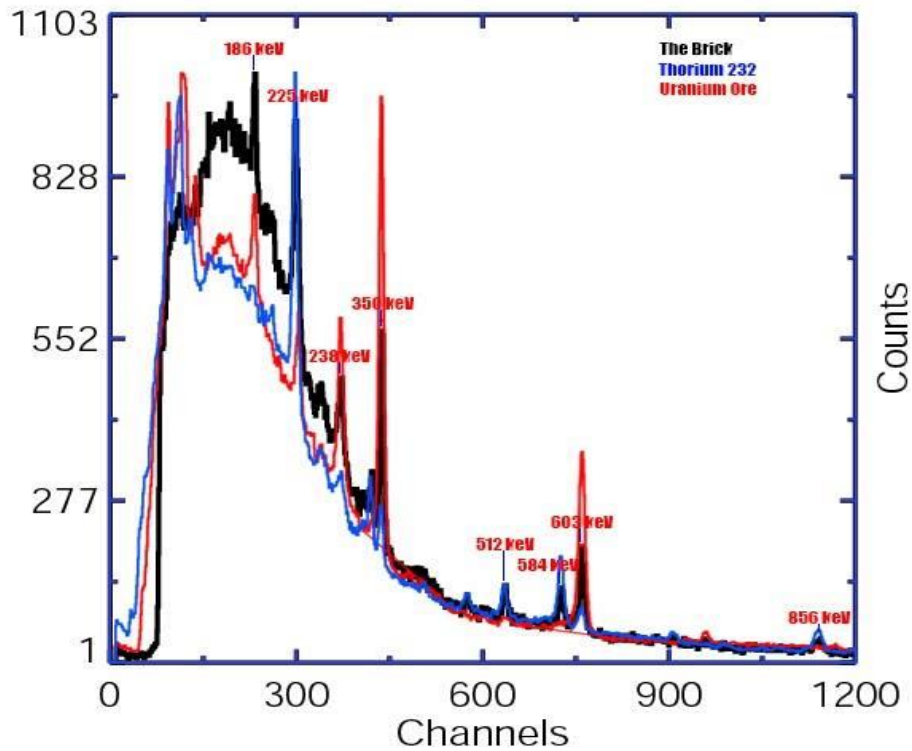


Figure 15. Spectrum of “Yoda the brick” overlapped with ^{238}U and ^{232}Th spectrums.

6) Conclusion. – The test results presented in this document prove that CZT can be a viable alternative for radiation detectors when compared to other semiconductor detectors. Data obtained from “Yoda the Brick” from both the CZT detector and the HPGe detector show that CZT can keep up with HPGe in terms of energy resolution, while at the same time offering room-temperature operation at a lower price due to CZT being cheaper.

The design approach for this system also shows that it is not necessary to buy high quality CZT crystals to obtain high energy resolution, as the arrays of virtual Frisch Grid detectors with 3-D corrections used in this device can detect several radiation sources at different positions with high energy resolution.

The brick situation proves the efficiency of this device, as well as it serves as a good example of the importance of this type of device as it proves that we can never know where and what can be a radioactive source. It also shows the range of applications this detector has in the field of nonproliferation and national security.

Acknowledgements

I want to thank all the people who made this opportunity possible for me. Starting with Dr, Deidra Hodges for considering me to be a part of this program. To our mentor Aleksey Bolotnikov for all the effort, the opportunities he has given us, and the knowledge he has passed down to us. To Luis Ocampo for his guidance at the beginning of the program. To Jose Gomera for allowing us to use his HPGe detector for our measurements. To the Department of Energy (DOE) and the Office of Educational Programs (OEP) for making this opportunity possible, and our sponsors the National Science Foundation (NSF) and the Louis Stokes Alliances for Minority Participation (LSAMP) office.

References

1. Glenn Knoll. *Radiation Detection and Measurement 3rd edition*. John Wiley & Sons Inc. 2000.
2. A. E. Bolotnikov, G. S. Camarda, G. De Geronimo, J. Fried, D. Hodges, A. Hossain, K. Kim, G. Mahler, L. Ocampo Giraldo, E. Vernon, G. Yang, R. B. James. *A 4x4 array module of position-sensitive virtual Frisch-grid CdZnTe detectors for gamma-ray imaging spectrometers*. 2018.